

Galactic Positron Production from Supernovae

P.A. Milne¹, M.D. Leising², L.-S. The²

1 NRC/NRL Resident Research Associate, Naval Research Lab, Code 7650, Washington DC 20375

2 Clemson University, Clemson, SC 29631

ABSTRACT The energy deposition into the ejecta of type Ia supernovae is dominated at late times by the slowing of positrons produced in the β^+ decays of ^{56}Co . Fits of model-generated light curves to observations of type Ia supernovae suggest that a significant number of positrons escape the ejecta and annihilate as a delayed emission. In this work, the isotopic yields of the β^+ decay unstable nuclei, ^{56}Co , ^{44}Ti & ^{26}Al are combined with the delayed annihilation fractions of each isotope for types Ia, Ib, II supernovae to generate an estimate of the positron production rate due to supernovae. It is shown that SN produced positrons can explain a sizeable fraction of the galactic positron annihilation radiation, as measured at 511 keV by the CGRO/OSSE, SMM and TGRS instruments.

1. INTRODUCTION

Supernovae (SNe), both thermonuclear and core collapse, have been suggested to be sources of galactic positrons through the β^+ decays of ^{56}Co , ^{44}Sc & ^{26}Al (Clayton 1973). The annihilation of these positrons can occur promptly (defined here as within a decade of the SN event) or can be delayed (defined here as $\sim 10^3$ years or more after the SN event). The annihilation of interest in this paper is the delayed emission where the integrated contributions from many SNe combine to produce a diffuse emission. The three isotopes, ^{56}Co , ^{44}Sc & ^{26}Al , have very different mean lifetimes and thus have different factors that determine what fraction of the total decay positrons annihilate as a delayed emission. In this paper we define the parameters relevant to quantifying the SN contribution to galactic positrons. We then estimate these parameters, comparing our values with previous estimates, and emphasizing which estimates have observational support. In particular, we show fits to the late light curves of type Ia SNe which suggest that a significant fraction of ^{56}Co positrons escape the SN ejecta to contribute a sizeable portion of the observed annihilation radiation.

Implicit in this entire study is the assumption that all SNe are approximated by the types Ia, Ib & II and that each type is homogeneous to the extent that a handful of models are adequate to describe the positron yield of the entire class. It is further assumed that the explosion kinematics and nucleosynthesis of current SN modeling is accurate enough that parameter ranges shown truly span the range of solutions. The goal of this paper is to estimate the SN contribution to galactic positron annihilation. To perform this estimate, SN rates used in this study are inferred from other galaxies. It is possible that the Galaxy has anomalous SN rates (as would occur if there has been a starburst at the galactic center within the last 10^6 years) or that there is leakage of positrons out of the Galaxy. Future 511 keV and 1.8 MeV maps (as well as maps of other nuclear decay lines) will be used to invert this problem and *determine* the recent galactic SN history. The current study is a consistency check as much as it is a solution to galactic positron production.

2. POSITRON YIELD PARAMETERS

The positron production rate per isotope, per SN type, is the product of the isotopic yield times the β^+ decay branching ratio, times the fraction of decay positrons which annihilate as a delayed emission, times the SN rate of that SN type. This product is then summed by isotope and by SN type to arrive at the total positron production rate. Assuming that the only relevant isotopes are ^{56}Co , ^{44}Sc & ^{26}Al , and that three SN types must be considered (types Ia, Ib & II), quantifying the SN positron production rate reduces to 9 isotopic yields, 9 delayed annihilation fractions, 3 branching ratios & 3 SN rates. The branching ratios and other β^+ decay parameters for the three decays are relatively well-known and are shown in Table 1. The most complete estimates of the other 21 parameters was performed in a paper by Chan & Lingenfelter (1993) (hereafter CL). They simulated positron

Table 1: **TABLE 1.** Parameters relevant to the positron-producing decays of ^{56}Co , ^{44}Sc & ^{26}Al .

Decay Chain	Mean Lifetime	Branching ratio	$\langle \text{KE}_{e^+} \rangle$ (MeV) ^a	$\text{KE}_{e^+}^{max}$ (MeV) ^b
$^{56}\text{Ni} \rightarrow ^{56}\text{Co} \rightarrow ^{56}\text{Fe}$	$8.8^d, 111^d$	0.19	0.64	1.46
$^{44}\text{Ti} \rightarrow ^{44}\text{Sc} \rightarrow ^{44}\text{Ca}$	$85.4^y, 6^h$	0.95	0.63	1.46
$^{26}\text{Al} \rightarrow ^{26}\text{Mg}$	$1.0 \times (10^6)^y$	0.82	0.47	1.14

^aMean kinetic energy of distribution of emitted positrons.

^bEndpoint energy of distribution of emitted positrons.

transport through SN models of all three types arriving at a number of conclusions. (1) For the β^+ decay of ^{26}Al , the mean lifetime is long-enough that ^{26}Al is a delayed emission source independent of positron transport physics. For ^{26}Al , the delayed fraction can be set equal to 1 for all three SN types. (2) The independent observation of 1.8 MeV line emission due to the de-excitation of $^{26}\text{Mg}^*$ produced in the $^{26}\text{Al} \rightarrow ^{26}\text{Mg}^*$ decay can estimate the ^{26}Al contribution (though not specifically the SN-produced ^{26}Al contribution) to galactic positron annihilation. (3) For ^{56}Co & ^{44}Sc decay positrons, the alignment and/or strength of the magnetic field must be considered when estimating the delayed annihilation fraction. For ^{44}Sc , the effect of the magnetic field varies from a $\leq 1\%$ effect (type Ia), to a 66% effect (type II). For ^{56}Co in type Ia SNe, the delayed annihilation fraction changes even more dramatically. (4) If the magnetic field characteristics are favorable to positron escape, then the decay of ^{56}Co produced in type Ia SNe may be the dominant contributor of galactic positrons. If not, then the dominant contributor of galactic positrons is from ^{44}Sc decays.

The critical parameter is thus the delayed annihilation fraction for ^{56}Co decays in type Ia SNe, which depends upon the magnetic field characteristics of the SN ejecta. CL assumed that the field strength is strong enough to confine positrons to the field lines, and estimated the positron survival for two opposite geometries. The first geometry assumes that the field is frozen into the ejecta and is combed to become essentially radial as the ejecta expands. Positrons spiral along the field lines experiencing mirroring/beaming, with a fraction of the positrons escaping the SN ejecta. The escaping positrons then enter a lower density medium and annihilate on longer timescales. This scenario will be referred to as the “radial” scenario ($l=\infty$ in CL terminology). The second geometry assumes that the field remains turbulent throughout the expansion of the SN ejecta. Positrons are trapped in the same location (in mass coordinates) as they are emitted. This scenario is referred to as the “trapping” scenario ($l=0$ in CL terminology), and the fraction of positrons that survive 10^3 years in the dense ejecta is much lower than the escape fraction in the radial scenario. Colgate et al. (1980) argued for a third, “weak field” scenario, where the field strength is inadequate to confine the positrons. In this scenario the positrons follow photon-like, straight line trajectories. Simulations have shown that the escape fractions and energy deposition rates for this scenario are approximately equal to the radial scenario (a result suggested by Colgate et al.). Throughout the remainder of this paper, only the terms radial and trapping will be used, but it is implied that radial represents radial or weak field solutions.

3. SN Ia LIGHT CURVES & POSITRON ESCAPE

CL calculated escape fractions from type Ia SNe for radial and trapping field geometries, but did not attempt to determine which scenario occurs in nature. They referred to the opposing conclusions of Colgate et al. (1980) and Axelrod (1980). Colgate et al. showed that energy deposition rates featuring positron escape could suitably explain the B band light curves of SN 1937C & SN 1972E. Axelrod argued for an alternative explanation, that no positron escape was evidenced, rather that the apparent deficit in the luminosity (relative to 100% positron trapping) was due to emission of an increased fraction of the deposited energy in unobservable infrared energy bands. This phenomenon was referred

to as an “infrared catastrophe” and has since been observed in the core collapse supernova, SN 1987A. Recent papers have been only somewhat successful in clarifying the picture. Cappellaro et al. (1997) and Ruiz-Lapuente et al. (1997) fit model-generated bolometric light curves to observations, both studies concluding that positron escape is favored in some, but not all cases. Fransson et al. (1996), after including a network of reaction rates, simulated multi-band light curves for the SN Ia model, DD4 (assuming positron trapping). They generated light curves which featured an “infrared catastrophe”, but which are in conflict with the light curves of SN 1972E (and all other late observations of SN Ia). None of these papers performed a detailed treatment of the positron transport, adapting photon transport codes instead.

Milne et al. (1999) explicitly treated both the gamma-photon and positron transport, assuming radial and trapping field geometries, and allowing for a range of ionizations (ranging from 1% ionization to triple ionization). A characteristic model-generated bolometric light curve of the model W7 is shown in Figure 1. Before $\sim 200^d$, positron lifetimes are short for all field and ionization assumptions, the light curves are identical with the zero lifetime (or instantaneous) light curve (In). With time, the SN ejecta expands and rarefies, increasing the positron lifetimes. In the radial scenario (R), the expansion leads to positron escape, and thus a deficit of energy deposition. As free electrons are more efficient at slowing positrons than are bound electrons, the low 1% ionization light curve features the maximum deficit from instantaneous annihilation. In the trapping scenario (T), the expansion permits non-zero lifetimes, but the majority of the energy is later deposited. At late times, the deposition of this stored energy makes the trapping light curves brighter than either the radial or the instantaneous light curves. For low 1% ionization, longer positron lifetimes lead to more energy being stored. The delayed deposition of this stored energy leads to brighter light curves at later times for low ionization solutions.

Bolometric light curves were generated for 22 SN Ia models. These models were selected to span Chandrasekhar, sub-Chandrasekhar and merger scenarios. The separation between radial and trapping light curves was found to exceed either the effects of model type or the level of ionization. These model-generated light curves were then fitted to the 10 SN Ia best observed at late times.¹ Of these 10 SNe, eight were considered either normal- or super-luminous. Of these 8, seven were suitably fitted with positron escape according to the radial field scenario. Five of the seven were better fitted with positron escape than with positron trapping. None were better fitted with positron trapping. The four best examples are shown in Figure 2, all 10 SNe are shown in Milne et al. (1999). The preference of positron escape is apparent in SNe 1992A (both bolometric (not shown) and V band, fit with DD23C (Höfllich et al. 1998)) & 1990N (fit with W7DN (Yamaoka et al. 1992)) without further explanation. For SN 1937C (fit with DET2 (Höfllich, Khokhlov, & Wheeler 1995)), B band data was used, thus fitting began after 120^d at which time color evolution has been empirically determined to cease in SN Ia. For SN 1991T (fit with HECD (Kumagai 1997)), the very late emission is dominated by a light echo, discovered spectrally by Schmidt et al. (1996) and imaged by HST (Boffi et al. 1998). Though the light curves for the range of ionizations (filled curves) are shown with a constant luminosity light echo included, the dashed and dot-dashed lines show the low ionization radial and trapping curves with no light echo. It is apparent that the trapping curves are already too bright without the additional emission from an echo, the radial curve suitably explains the data before 480 days. This suggests a light echo that “turns on” after 480 days, which would occur if the light echo is due to the peak light sweeping through an off-axis cloud. The asymmetry of the HST image would appear to permit that interpretation.

The conclusion of Milne et al. (1999) is that the late light curves of normal- and super-luminous type Ia SNe can be suitably explained with positron escape. Though the sample is neither large enough, nor well-enough observed to rule out trapping in all cases, the lack of counter-examples suggest escape to be the dominant result. Many of the SNe used in that study were also used in the studies of Cappellaro et al. (1997), Ruiz-Lapuente et al. (1997) & Fransson et al. (1996). Milne et al. (1999) did not find positron trapping to be favored for any SN, in mild disagreement with some of the conclusions of these earlier studies. Based upon these observations, the positron escape fractions claimed in Milne et al. (1999) will be inserted into the ^{56}Co -SN Ia portion of the positron production

¹Discussions regarding the validity of fitting model-generated energy deposition rates to observed band photometry and/or “uvoir” bolometric light curves are given in Milne et al. (1999).

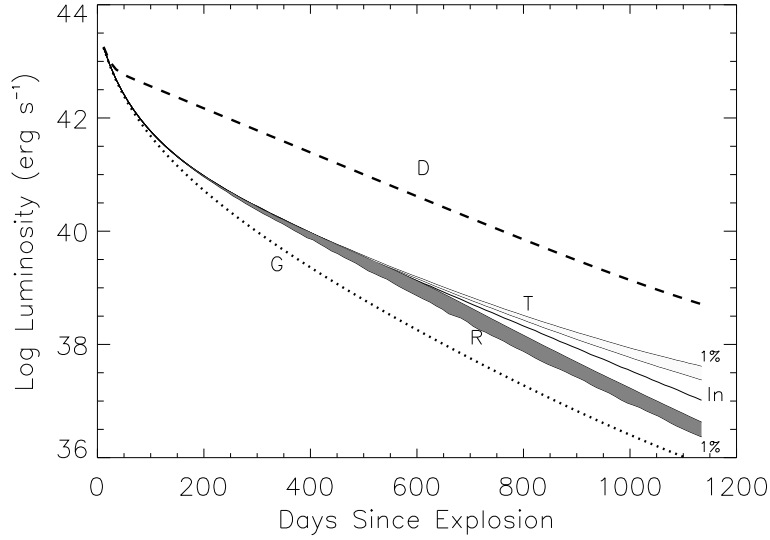


Figure 1: **FIGURE 1.** A model-generated bolometric light curve of the model W7. The dashed line (D) assumes instantaneous deposition of all decay energy. The dotted line (G) uses the results of the gamma energy deposition only and assumes no deposition of positron energy. Between these two boundaries are the results of the gamma energy deposition coupled with instantaneous positron deposition (thick line, In) and the range of curves for a radial field geometry (dark shading, R) and for a trapping geometry (light shading, T) as the electron ionization fraction varies from $0.01 \leq \chi_e \leq 3$.

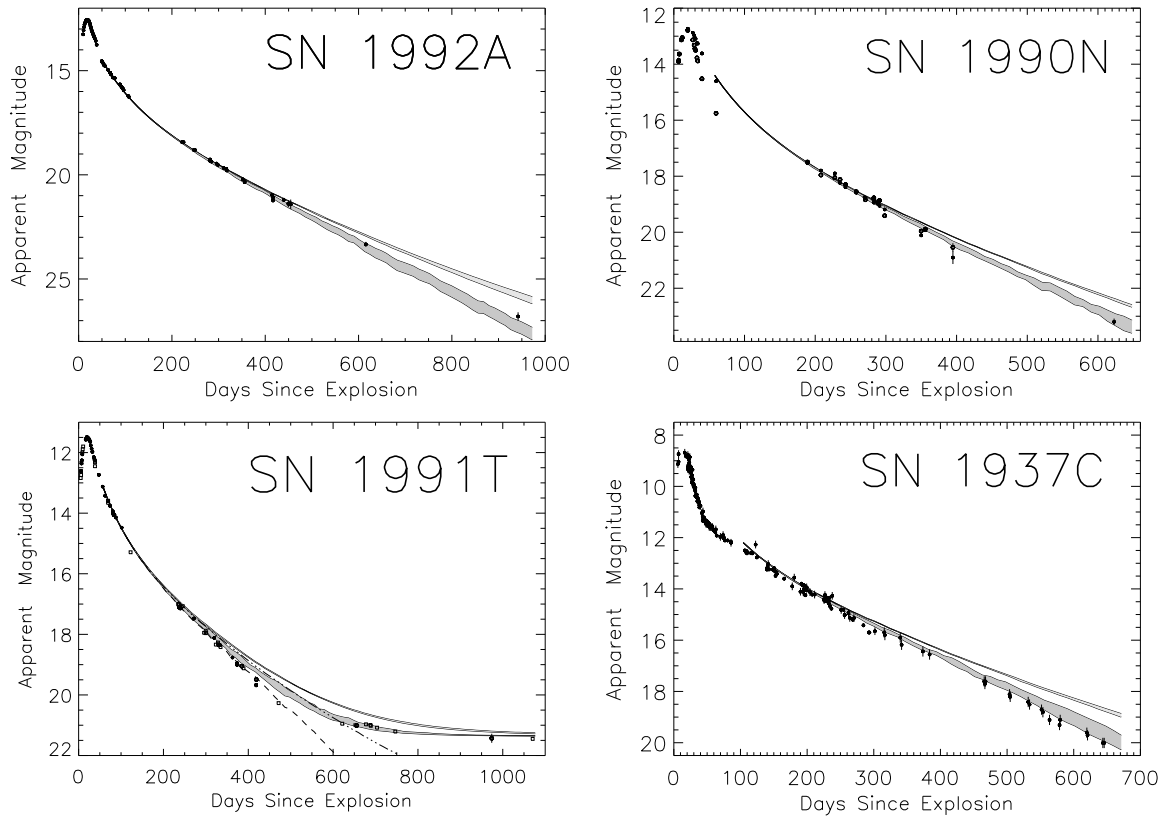


Figure 2: **FIGURE 2.** Model-generated light curves fit to the V and B band light curves of four type Ia SNe; SN 1992A (V: Suntzeff 1996), SN 1990N (B&V: Lira et al. 1998), SN 1991T (V: Lira et al. 1998, Cappellaro et al. 1997, Schmidt et al. 1994) & SN 1937C (B: Schaefer 1994). The light curves are better explained by radial escape (dark shading) than by positron trapping (light shading). The model-generated light curves of SN 199T are shown with a constant luminosity light echo added, the same curves without a light echo are displayed with dashed (radial) and dot-dashed (trapping) lines.

rate calculations rather than the trapping-radial range suggested by CL. The determination of the escape of ^{56}Co positrons from type Ia SNe was based upon the existence of a “positron phase”, an epoch during which the energy deposition is dominated by the slowing of positrons. This “positron phase” does not occur in core collapse SNe, due to the more efficient trapping of gamma-photons. The dominance of ^{56}Co decay photons transitions to the dominance of ^{57}Co decay photons without an epoch of positron dominance. Since no determination of the field characteristics of types Ib and II SNe are possible, the trapping-radial ranges claimed by CL are used in section 5.

4. ISOTOPIC YIELDS

The SN Ia delayed annihilation fraction may prove to be the most critical parameter for quantifying positron production from SNe, but twenty other parameters must also be estimated. The other eight delayed annihilation fractions were adequately approximated by CL, the nine isotopic yields and three SN rates remain undetermined.

The isotopic yields of ^{56}Ni (the parent isotope of ^{56}Co) are the best constrained. In all three SN types, energy deposition from the ^{56}Ni and subsequent ^{56}Co decays power the light curves. This allows fits of model-generated bolometric light curves to observations, combined with distance estimates to the host galaxy, to constrain the ^{56}Ni yields. Type Ia SNe produce the most ^{56}Ni per SN event, ranging from 0.3 -0.9 M_{\odot} in various SN Ia models. Diehl (1997) suggests the typical ^{56}Ni yield to be 0.5 M_{\odot} . As shown by Milne et al. (1999), the larger nickel yield in Chandrasekhar mass models partially compensates for the lower escape fraction (relative to sub-Chandrasekhar mass models), leading to the positron yields being virtually independent of the progenitor mass. The SN Ia ^{56}Ni yield estimate is also influenced by the existence of super- and sub-luminous classes. An additional result of Milne et al. (1999) is the acceptance of both Chandrasekhar mass and sub-Chandrasekhar mass explanations for normally- and super-luminous SNe Ia, but rejection of all currently proposed models for sub-luminous SNe Ia. CL discussed a “Ip” model class as an explanation for sub-luminous SNe Ia. The Ip model class featured large positron yields. This work will not include that class due to the findings of Milne et al. (1999).

The ^{56}Ni yields from type II SNe are well-constrained due to the observations of the nearby SN 1987A. That SN produced 0.08 M_{\odot} of ^{56}Ni , the fiducial value used by Dermer & Skibo (1997). The type Ib ^{56}Ni yield is taken from CL, ranging from 0.08 -0.28 M_{\odot} . Diehl (1997) estimates the type II/Ib ^{56}Ni yield to be 0.1 M_{\odot} . The type II/Ib ^{56}Ni yields are of little importance due to the low delayed annihilation fractions for these SNe.

The isotopic yields of ^{44}Ti are obtained from the outputs of SN models (with fewer observational constraints) and are poorly constrained. Timmes et al. (1996) show a range of ^{44}Ti yields for core collapse models, claiming $3 \times 10^{-5} M_{\odot}$ (type II) & $6 \times 10^{-5} M_{\odot}$ (type Ib) to be typical values, but later tripling these yields in a positron production calculation. Nomoto (1997) suggests that type II SNe produce $5 \times 10^{-5} M_{\odot}$ of ^{44}Ti , in agreement with the value used by Diehl (1997) for types II/Ib. Meyer et al. (1995) estimates the ^{44}Ti yield from a 25 M_{\odot} SN to be $1.5 \times 10^{-4} M_{\odot}$. The $^{44}\text{Ti} \rightarrow ^{44}\text{Sc} \rightarrow ^{44}\text{Ca}$ decay has been directly observed in the Cas A SNR (type II or Ib) via the 1.157 MeV de-excitation line of ^{44}Ca and the 68 keV and 78 keV de-excitation lines of ^{44}Sc . From measurements taken by the CGRO/COMPTEL, the CGRO/OSSE and the *Rossi X-Ray Timing Explorer* High Energy X-Ray Timing Experiment, the ^{44}Ti yield is estimated to be $2.2 \times 10^{-4} M_{\odot}$ (The et al. 1998, using the 85^y ^{44}Ti mean lifetime from Ahmad et al. 1997). The SN Ia ^{44}Ti yields are equally uncertain. The Chandrasekhar mass model, W7 (Nomoto, Theilemann & Yokoi 1984), produces $\sim 1.8 \times 10^{-5} M_{\odot}$ of ^{44}Ti . The low mass portion of sub-Chandrasekhar mass models produce more ^{44}Ti , ranging from $(2-40) \times 10^{-4} M_{\odot}$ (Woosley & Weaver 1994), though these low mass examples cannot explain 100% of SN Ia events due to nucleosynthesis considerations. Dermer & Skibo (1997) use the CL results, scaling the ^{44}Ti yield with the ^{56}Ni yields. This leads to $(3-8) \times 10^{-5} M_{\odot}$, $1.7 \times 10^{-4} M_{\odot}$ & $\leq 2.0 \times 10^{-4} M_{\odot}$ per SN for types Ia, Ib, II respectively.

The isotopic yield of ^{26}Al in type Ia SNe is very low ($\sim 10^{-6}$ -Diehl 1997). In core collapse SNe, estimates of the yields range from $2 \times 10^{-4} M_{\odot}$ (for SN II/Ib -Diehl 1997) to $(0.3 -20) \times 10^{-5} M_{\odot}$ (for SN II -Prantzos 1996). Timmes & Woosley (1997) suggest the mass function averaged ^{26}Al yield per core collapse SN event is $7.7 \times 10^{-5} M_{\odot}$.

4. SUPERNOVA RATES

Estimation of SN rates in the Galaxy is dependent upon the collective SN rates from other spiral galaxies.² The SN rates from SN surveys are given in units of $10^{10} L_{\odot}^B$ and scaled to $2.3 \times 10^{10} L_{\odot}^B$. The differences between suggested rates is due to different algorithms accounting for selection effects. The SN Ia rate is relatively well-constrained, estimates are 0.4 ± 0.1 (Cappellaro et al. 1997), 0.28 (Tammann et al. 1994), 0.5 (Hatano et al. 1997). The SN Ib rate is approximately equal to the SN Ia rate, but the estimates are more varied. Estimates are 0.2 ± 0.1 (Cappellaro et al. 1997), 0.8 (Hatano et al. 1997), 0.3 (Tammann et al. 1994). The SN II rate is the largest of the three and the most varied. Estimates are 1.2 ± 0.6 (Cappellaro et al. 1997), 3.8 (Hatano et al. 1997), 1.5 (Tammann et al. 1994).

5. POSITRON PRODUCTION RATES

Shown in Table 2 are the parameters relevant to estimating the galactic positron production rate from SNe. In many cases, the most favorable positron yields per SN event, as shown in column (6), are realized only by anomalous SNe, and would have large recurrence times. As seen in columns (6) and (7), SN Ia ^{56}Co decays yield the most positrons per SN and per second. The ^{56}Co decay contributions from SN Ib & II are zero due to rejecting the 100% mixing scenario allowed by CL. The ^{44}Ti decay contributions (per second) are not negligible. The favorable ^{44}Ti yields cannot be claimed for all three SN types simultaneously, as that would lead to anomalously large $^{44}\text{Ca}/^{56}\text{Fe}$ production. The largest ^{44}Ti decay contribution would result if a considerable fraction of all SN Ia events are low-mass sub-Chandrasekhar explosions, and core collapse SNe possess radial (or weak) magnetic fields. The ^{26}Al decay contribution is dominated by core collapse SNe. The positron yield per second is better estimated by including results of measurements of the 1.8 MeV line emission. In 82% of $^{26}\text{Al} \rightarrow ^{26}\text{Mg}$ decays, both a positron and a 1.8 MeV line photon are produced. Core collapse SNe have been suggested to account for as much as 100% of galactic ^{26}Al (Timmes et al. 1997). Assuming the entire emission to emanate from core collapse SNe at the distance of the galactic center (~ 8 kpc distant), reported 1.8 MeV central radian fluxes of $3 \times 10^{-4} \text{ ph cm}^{-2} \text{ s}^{-1}$ (Knodlseder et al. 1999) translates to $1.9 \times 10^{42} \text{ e+ s}^{-1}$, approximately equal to the ^{44}Ti decay production rate.

The total positron production rates are $1.0 \times 10^{43} \text{ e+ s}^{-1}$ for ^{56}Co decays, $2.4 \times 10^{42} \text{ e+ s}^{-1}$ for ^{44}Ti decays, and $1.9 \times 10^{42} \text{ e+ s}^{-1}$ for ^{26}Al decays. These values are in general agreement with estimates by Timmes et al. (1996), who derived the values $1.6 \times 10^{43} \text{ e+ s}^{-1}$, $4.5 \times 10^{42} \text{ e+ s}^{-1}$, and $2.9 \times 10^{42} \text{ e+ s}^{-1}$ respectively. Notably different is the ^{44}Ti yield. In that study, it was erroneously suggested that two positrons are generated in 95% of $^{44}\text{Ti} \rightarrow ^{44}\text{Sc} \rightarrow ^{44}\text{Ca}$ decays (a single positron is generated). That study also tripled the ^{44}Ti yields in all three SN types to permit their chemical evolution model to match the solar ^{44}Ca abundance, but used the lower delayed annihilation fraction (34% rather than the value 99% used in this study). The net difference is that the ^{44}Ti yields in Timmes et al. (1996) are roughly double the values claimed here. The difference in ^{26}Al decay yield may be due to a different 1.8 MeV total flux.

Assuming a constant SN rate over the last 10^6 years, steady-state positron production/annihilation and no leakage of positrons from the Galaxy, the above production rate can be compared with the 511 keV line flux. A positron production rate of $1.4 \times 10^{43} \text{ e+ s}^{-1}$ would generate a 511 keV flux of $1.1 \times 10^{-3} \text{ ph cm}^{-2} \text{ s}^{-1}$ if emitted from the galactic center (~ 8 kpc distant) and annihilating with a positronium fraction of 0.95. That is about 1/3 - 1/2 of the total 511 keV flux suggested by CGRO/OSSE, SMM & TGRS measurements (Milne et al. 1999b). Correcting this value to a distributed emission has not been performed.³

²Estimates of the galactic SN rate from the historical record, from surveys of supernova remnants, and from galactic nucleosynthesis are considered to be less reliable than assuming the Galaxy to be an Sb galaxy and assuming that the SN rates scale with L^B .

³Timmes et al. (1997) quoted a positron production rate of $1.5 \times 10^{-3} \text{ e+ s}^{-1}$ from 511 keV measurements, that value is too low by a considerable fraction.

Table 2: **TABLE 2.** Galactic positron production rates from SNe. Italicized values denote preferred values from a range.

SN Type	SN Rate ^(a)	Isotope	Isotopic Yield (M _⊙)	Delayed Ann. Frac.	[per SN] ^(b)	Positron Yield [per s] ^(c)
(1)	(2)	(3)	(4)	(5)	(6)	(7)
Ia	0.4±0.1	⁵⁶ Ni	<i>0.5(0.2-0.8)</i>	0.001-0.11	<i>8(1-20)^(d)</i>	<i>1.0(0.8-1.3)</i>
		⁴⁴ Ti	<i>(0.2-12) x 10⁻⁴</i>	0.99	0.04-3.8	<i>0.01-0.49</i>
		²⁶ Al	<i>10⁻⁶</i>	1.00	4 x 10 ⁻³	<i>4 x 10⁻⁴</i>
Ib	0.3 ^{+0.5} _{-0.1}	⁵⁶ Ni	0.18±0.10	0.0	0.00	0.00
		⁴⁴ Ti	<i>(6-22) x 10⁻⁵</i>	0.85- <i>0.99</i>	0.1-0.4	<i>0.01-0.29</i>
		²⁶ Al	<i>0.8(0.3-20) x 10⁻⁴</i>	1.00	0.01-0.91	<i>0.03(0.00-0.23)</i>
II	3.1 ^{+0.7} _{-1.9}	⁵⁶ Ni	0.08-0.28	0.0	0.00	0.00
		⁴⁴ Ti	<i>(3-22) x 10⁻⁵</i>	0.34- <i>0.99</i>	0.03-0.62	<i>0.21(0.01-0.79)</i>
		²⁶ Al	<i>0.8(0.3-20) x 10⁻⁴</i>	1.00	0.01-0.91	<i>0.30(0.00-1.11)</i>

^(a) The SN rate is in units of SNe per century.

^(b) The yields per SN are in units of 10⁵² positrons SN⁻¹.

^(c) The yields per second are in units of 10⁴³ positrons s⁻¹.

^(d) The SN Ia yield per SN is the from Milne et al. (1999), rather than the product of SN Ia parameters.

6. DISCUSSION

The positrons produced in the β^+ decays of ^{56}Co , ^{44}Ti & ^{26}Al have been shown to potentially contribute a large fraction of the total galactic positron production rate. This work shows observational support for the suggestion made by Chan & Lingenfelter (1993) that significant numbers of ^{56}Co decay positrons can escape from the ejecta of type Ia SNe. Observations of supernovae and supernova remnants, combined with improved nucleosynthesis modeling has led to improved constraints upon the various parameters that determine SN positron production.

A future step in modeling the galactic positron production rate from SNe will be to compare spatial distributions with CGRO/OSSE measurements of 511 keV positron-electron annihilation radiation. Type II/Ib SNe are seen only in the disks of spiral galaxies, type Ia SNe occur in both bulges and disks. More progress must be made towards understanding both the intrinsic B/D ratios of type Ia SNe in spiral galaxies, and the B/D ratio measured in the 511 keV emission before useful comparisons can be made.

An observation that would solidify the picture of SN positron production would be the detection of 511 keV emission from nearby SNe. In type Ia SNe, detection of emission above the level expected for ^{44}Ti decays would be evidence of positron escape. In all SN types, the intensity and distribution of the emission would trace the diffusion of positrons from the remnant into the Galaxy. Additionally, the detection of prompt positron annihilation in SNe would better constrain isotopic yields and delayed annihilation fractions. The late light curves of SNe Ia suggest positron escape, but more observations are required to accurately quantify the positron yields. If all these observations are made, the hypothesis of SN production of galactic positrons will be demonstrated and positron annihilation radiation measurements can be used to probe the recent SN history in the Galaxy.

REFERENCES

- Ahmad, I. et al. 1997, Phys. Rev. Lett., 80, 2550
Axelrod, T.S. 1980, Ph.D.thesis, Univ. California at Santa Cruz
Boffi, F.R. et al. 1998, BAAS, 192, 6.07
Cappellaro, E., et al. 1997a, A & A, 322, 431
Cappellaro, E., et al. 1997b, A & A, 328, 203
Chan, K.-W., Lingenfelter, R. 1993, ApJ, 405, 614
Clayton, D.D. 1973, Nature, 244:139, 137
Colgate, S., Petschek, A.G., Kreise, J.T. 1980, ApJ, 237, L81
Dermer, C.D., Skibo, J.G. 1997, ApJ, 487, L57
Diehl, R. 1997, in Proceedings of the 2nd INTEGRAL Workshop, 9
Fransson, C., Houck, J., Kozma, C. 1996, in IAU Colloq. 145, Supernovae and Supernova Remnants, ed. R. McCray & Z. Wang (Cambridge: Cambridge University Press), 41
Hatano, K., Fisher, A., Branch, D. 1997, 290, 360
Hófflich, P., Khokhlov, A., Wheeler, J.C. 1995, ApJ, 444, 831
Hófflich, P., Wheeler, J.C., Theilemann, F.-K. 1998, ApJ, 495, 617
Knodlseder, J., et al. 1999, A & A, 344, 68
Kumagai, S. 1997, private communication
Lira, P. et al. 1998, AJ, 115, 234
Meyer, B.S., Weaver, T.A., Woosley, S.E. 1995, Meteoritics, 30, 325
Milne, P.A., The, L.-S., Leising, M.D. 1999, ApJS, 124, 503
Milne, P.A., et al. 1999b, these Proceedings, ,
Nomoto, K., Theilemann, F.-K., Yokoi, K. 1984, ApJ, 286, 644
Nomoto, K., et al. 1997, Nuclear Physics A, 621, 467
Prantzos, N., Diehl, R. 1996, Phys. Rep., 267, 1
Ruiz-Lapuente, P., Spruit, H. 1997, ApJ, 500, 360
Schaefer, B.E. 1994, ApJ, 426, 493
Schmidt, B.P. et al. 1994, ApJ, 434, L19
Sunzteff, N.B. 1996, in IAU Colloq. 145, Supernovae and Supernova Remnants, ed. R. McCray & Z. Wang (Cambridge: Cambridge University Press), 41
Tammann, G.A., Löffler, W., Schröder, A. 1994, ApJS, 92, 487

The, L.-S., et al. 1998, ApJ, 504, 500
Timmes, F.X., et al. 1996, ApJ, 464, 322
Timmes, F.X., Diehl, R., Hartmann, D.H. 1997, ApJ, 479, 760
Timmes, F.X., Woosley, S.E. 1997, ApJ, 481, L81
Yamaoka, H., et al. 1992, ApJ, 393, L55